TURBULENT CHARACTERISTICS OF DISCHARGE FLOW FROM THE TURBINE IMPELLER*

Jan DRBOHLAV[a], Ivan FOŘT[b], Karel MÁCA[c] and Jan PTÁČEK[b]

[a] *Dairy Research Institute, 110 00 Prague 1*
[b] *Department of Chemical Engineering, Prague Institute of Chemical Technology, 166 28 Prague 6 and*
[c] *Institute for Hydrodynamics, Czechoslovak Academy of Sciences, 166 00 Prague 6*

Received March 11th, 1977

Experimental characteristics are presented in the paper of the turbulent velocity field in the discharge stream from the rotating standard six-blade turbine impeller with disc in a cylindrical vessel equipped with four radial baffles. Experimental results (in the form of radial, tangential and axial mean velocity components, corresponding square roots of the mean square fluctuation velocities and correlations for the significant velocity components) are compared with those of a phenomenological model viewing the rotating turbine impeller as a cylindrical tangential jet. The proposed model has been confirmed experimentally and permits predictions of the principle characteristics of the mean as well as fluctuation (turbulent) motion in the stream between the rotating impeller and the wall for common arrangements of mixing system with the turbine impeller ($d/D = 1/3, 1/4$).

Velocity field in the stream of liquid streaking from the space occupied by the rotating standard turbine impeller in a system with radial baffles markedly affects not only the flow in the batch as a whole but plays also an important role in the control of those phenomena influenced by mechanical mixing. The first task therefore is to solve the equation of motion for the region of the stream jet in order to obtain information about the flow in the remaining parts of the system.

Turbulent characteristics in the mixed system in question have been studied experimentally by several methods: Most authors used hot-wire or hot-film thermoanemometers in liquid[3,5,8,9,11,13,14] or air[6,7,12]. Others applied tracer techniques[4,10,21]. As far as the theoretical description of the turbulent velocity field in the examined stream is concerned, as the most advanced appears the one used by Van't Riet and coworkers[14]. These authors considered periodical pulsations of velocity induced by rotation of the turbine impeller. Because the former approach, although very correct and realistic, does not lead to a quantitative description of the examine stream the phenomenological approach viewing the impeller as a tangential cylindrical jet was preferred. Also, as already mentioned, this approach can serve as a basis for a quantitative description of the velocity field in the whole volume of the batch.

* Part IL in the series Studies on Mixing; Part XLVIII: This Journal *43*, 696 (1978).

THEORETICAL

Consider a mixed system with a standard six-blade turbine impeller with a disc located in the axis of a cylindrical vessel equipped with radial baffles on the wall (Fig. 1).

Fig. 2 sketches part of the mixed system and its frame of reference and clarifies also some more important quantities. Position of a point in the mixed system is set by the following cylindrical coordinates r, z, α_0. The mean velocity vector in the just defined point within the batch is given by its magnitude and the direction, the later being given by the angles α, β. The angle α is the angle made by the velocity vector and its projection onto the horizontal plane passing through the measuring point. β is the angle between the above projection and the straight line passing through the measuring point in the radial direction. The quantities $\bar{w}_r$, $\bar{w}_{tg}$, $\bar{w}_{ax}$ are components of the mean velocity vector. Description of the velocity field in the stream ejected by the rotating impeller starts from the equation of continuity and the Reynolds equation[1-3] for the bulk motion under the turbulent regime. It is assumed that the turbine impeller in the role of the source of motion may be replaced by an axially symmetric cylindrical slot – the tangential cylindrical jet. The liquid discharging from such a jet has the only non-zero velocity component in the tangential direction and merges with the liquid at rest and of infinite extent.

Analytical solution of the above mentioned two equations after introduction of eight simplifying assumptions and two boundary conditions leads to a three-para-

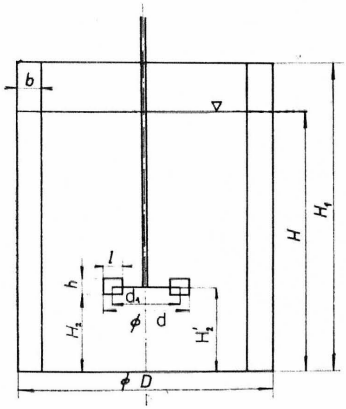

FIG. 1

Mixed System with Turbine Impeller (h/d = = 0·20; l/d = 0·25; d_1/d = 0·75)

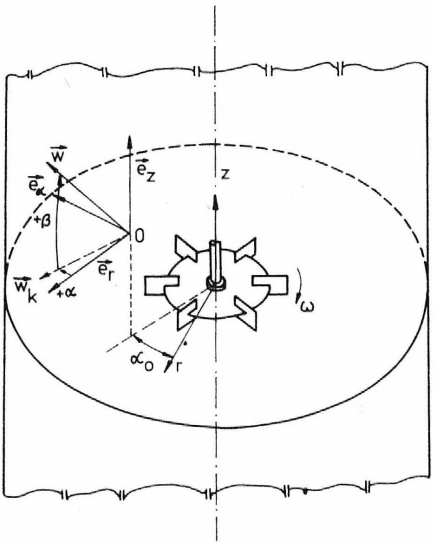

FIG. 2

Mixed System and Frame of Reference

meter equation expressing the dependence of the radial mean velocity component, $\bar{w}_r$, on the axial coordinate, z, further, to the relationship between the radial and tangential component of mean velocity. Since in the already cited paper[1] attention has been paid primarily to the bulk flow in the examined stream we shall confine ourselves here to a review of the obtained equations provided in Table I. Table II then contains definition sof the dimensionless quantities: the coordinates R and Z and the mean velocity components $\overline{W}_j$, $(j = r, tg, ax)$ considered as variables in Table I. The resulting three-parameter equation expresses the two-dimensional velocity

TABLE I

Characteristics of the Velocity Profile in the Discharge Stream from by the Turbine Impeller by the Parameters of Model: $A_1 = 0{\cdot}82(1 - R)$, $A_2 = 2{\cdot}63 - 3{\cdot}26R$, $A_3 = b_3R$, $H_2'/H = 1/2$: $b_3 \neq 0$, $H_2'/H = 1/3$: $b_3 = 0{\cdot}74$, $\sigma = 11{\cdot}2$, $A/2\pi\, dn = 0{\cdot}035$ m, $a = 0{\cdot}34$ d

I	*II*

Mean direction of flow: $\beta = 0$, $\alpha = \arcsin(a/r)$

Mean velocity

$$\overline{W}_r = A_1\{[1 - \mathrm{tgh}^2\, A_2(Z - A_3)]\} \qquad \overline{W}_r = \frac{A}{2\pi dn}\left(\frac{\sigma}{r^3}\right)^{1/2}(r^2 - a^2)^{1/4} \,.\, \{1 - \mathrm{tgh}^2\,[(h\sigma/4r)(Z - A)]\}$$

$$\overline{W}_{tg} = \overline{W}_r \,\mathrm{tg}\,\alpha\,, \quad \overline{W}_{ax} = 0\,, \quad \overline{W} = \overline{W}_r^2 + \overline{W}_{tg}^2$$

Dimensionless stream function

$$\psi = \frac{\pi hr}{2d^2}\frac{A_1}{A_2}\,\mathrm{tgh}\,[A_2(Z - A)_3] \qquad \psi = \frac{A}{nd^3}\left(\frac{r}{\sigma}\right)^{1/2}(r^2 - a^2)^{1/4} \,.\, \mathrm{tgh}\left[\frac{\sigma h}{4r}(Z - A_3)\right]$$

Turbulent characteristics

$$\varepsilon = \frac{A}{2}\,\frac{1}{(\sigma^3 r)^{1/2}}\,\frac{2r^2 - a^2}{(r^2 - a^2)^{3/4}}$$

$$\bar{\tau}_{r,ax} = -\frac{2\pi dn}{h}\,\varrho\varepsilon\, 8A_1A_2\,\frac{\exp[-2A_2(Z - A_3)]}{\{1 + \exp[-2A_2(Z - A_3)]\}^2}\,\mathrm{tgh}\,[A_2(Z - A_3)]$$

$$\bar{\tau}_{tg,ax} = \bar{\tau}_{r,ax}\,\mathrm{tg}\,\alpha\,, \quad \bar{\tau} = (\bar{\tau}_{tg,ax}^2 + \bar{\tau}_{r,ax}^2)^{1/2}$$

field in the examined stream while the parameters A_1, A_2, A_3 as well as σ and $A/\pi dn$ must be found from experimental velocity profiles $\overline{W}_r = \overline{W}_r(Z)$, ($R$ = const.). The parameter a, the so-called radius of the cylindrical tangential jet, is found from the known direction, alpha, of the mean velocity vector in the examined stream[1]. Physical significance of the parameters A_1, A_2, A_3 follows from the explicit form of the mean velocity profile $\overline{W}_r = \overline{W}_r(Z)$, (R = const.), (see also the right hand part of Table I): The parameter A_1 represents maximum radial velocity component of liquid on a given profile normalized by the peripheral velocity of the outer edges of the blades, πdn; the parameter A_2 is associated with the width of the stream jet in a given position, normalized by the width of the blade, h. The parameter A_3 expresses the dimensionless axial coordinate of the maximum on the velocity profile, *i.e.* its shift off the horizontal plane of symmetry of the turbine impeller.

All discussed parameters, apart from the quantities σ and $A/\pi dn$, have been assigned a linear dependence on the dimensioneless radial coordinate R whose constants were evaluated from experimental data. The proposed phenomenological model enables values to be determined of the important turbulent characteristics of the stream streaking from the turbine impeller: The eddy viscosity ε (regarded constant for the given radial distance r or R) and significant components of the turbulent stress tensor $\bar{\tau}_{r,ax}$ and $\bar{\tau}_{tg,ax}$ (regarded to be an order of magnitude higher than the

TABLE II

Definitions of Dimensionless Quantities and Transformations for Mean Velocity Components and Fluctuation Velocities from Experimental Data

Dimensionless variables

$$R = (r - a)/r\,, \quad Z = 2z/h\,, \quad \overline{W}_j = \bar{w}_j/\pi dn\,; \quad j = r, \mathrm{tg}, \mathrm{ax}$$

$$\overline{W'_j W'_{ax}} = \overline{w'_j w'_{ax}}/(\pi dn)^2\,; \quad j = r, \mathrm{tg}$$

Transformations

$$\bar{w}_r = \bar{w}\cos\alpha\cos\beta\,, \quad \bar{w}_{tg} = \bar{w}\cos\beta\sin\alpha\,, \quad \bar{w}_{ax} = \bar{w}\sin\beta$$

$$(\overline{w'^2_r})^{1/2} = ((\overline{w'^2})^{1/2}\cos\beta - (\overline{u'^2})^{1/2}\sin\beta)\cos\alpha$$

$$(\overline{w'^2_{tg}})^{1/2} = ((\overline{w'^2})^{1/2}\cos\beta - (\overline{u'^2})^{1/2}\sin\beta)\sin\alpha$$

$$(\overline{w'^2_{ax}})^{1/2} = (\overline{w'^2})^{1/2}\sin\beta + (\overline{u'^2})^{1/2}\cos\beta$$

$$\overline{w'_r w'_{ax}} = \overline{u'u'}\cos\alpha\,, \quad \overline{w'_{tg} w'_{ax}} = \overline{w'u'}\sin\alpha$$

corresponding components of the viscous stress tensor). In view of the relations

$$\bar{\tau}_{r,ax} = \varrho\varepsilon\, \partial\bar{w}_r/\partial z\,, \quad \bar{\tau}_{r,ax} = -\overline{\varrho w'_r w'_{ax}} \qquad (1), (2)$$

the appropriate component of the turbulent stress tensor can be used to determine the correlation $\overline{w'_r w'_{ax}}$ of the fluctuation components of velocity. Let us note that the last mentioned turbulent characteristic plays an important role in the calculation of the rate of dissipation of mechanical energy in the examined stream[4].

EXPERIMENTAL

The experiments were designed so as to provide a test of adequacy of the proposed model. The experiments were carried out in a cylindrical vessel equipped at the wall with four symmetrically located baffles (Fig. 1) and the standard six-blade disc turbine impeller[15] rotating in the axis of the vessel.

Geometrical characteristics as well as the experimental conditions are summarized in Table III.

The sequence of experimental examinations of the characteristics of the velocity field was as follows: *1*) Using the five-hole directional Pitot tube (Fig. 3) values of directional functions[20]

$$\varphi_1[\alpha(\alpha_1, \beta_1), \beta(\alpha_1, \beta_1)] = \frac{\bar{p}_1 - \bar{p}_3}{\bar{p}_0 - (\bar{p}_1 + \bar{p}_3)/2} \qquad (3)$$

and

$$\varphi_2[\alpha(\alpha_1, \beta_1), \beta(\alpha_1, \beta_1)] = \frac{\bar{p}_2 - \bar{p}_4}{\bar{p}_0 - (\bar{p}_2 + \bar{p}_4)/2} \qquad (4)$$

were found by calibration in the form

$$\varphi_1 = -(0{\cdot}0023\beta_1^2 + 2{\cdot}17)\,\mathrm{tg}\,2\alpha_1\,, \quad \varphi_2 = -2{\cdot}26\,\mathrm{tg}\,2\beta_1\,. \qquad (5), (6)$$

The quantities $\bar{p}_i$, $(i = 0, 1, 2, 3, 4)$ appearing in Eqs (*3*) and (*4*) are pressure differences read on the manometers connected to individual openings of the Pitot tube referred to values found at zero velocity of the flow past the probe. α_1 and β_1 are angles between the axis of the probe

TABLE III

Experimental Set-Up and Experimental Conditions ($H = D = 1$ m, $H'_2 = 0{\cdot}333$ m, $b = 0{\cdot}1$ m; water at 20°C; $d = 0{\cdot}250$ m; $d/D = 1/4$; $n = 140\ \mathrm{min}^{-1}$; $\mathrm{Re_M} = 1{\cdot}46 \cdot 10^5$. $d = 0{\cdot}333$ m $d/D = 1/3$; $n = 90\ \mathrm{min}^{-1}$; $\mathrm{Re_M} = 1{\cdot}66 \cdot 10^5$)

r, m	0·128	0·170	0·208	0·250	0·290	0·333
$R(d/D = 1/4)$	0·156	0·365	0·481	0·568	0·628	0·678
$R(d/D = 1/3)$	—	0·188	0·337	0·448	0·524	0·586

and the direction of the mean velocity vector at the measuring point; its relation to the angles α and β is given by the so-called Euler transformations[3]. *2)* In the next stage values of the mean velocity $\overline{w}$ at the measuring point were measured as well as the square roots of the mean square velocity components in the longitudinal and lateral direction, $\sqrt{\overline{w'^2}}$ and $\sqrt{\overline{u'^2}}$. Using the knowledge of the direction of the mean velocity vector (given by the angles α, β) the measurements were carried out with the hot-film probes[16] of the anemometer DISA-type 55M 01[17,18]. The method of measurement was described in detail in the cited work[3], or the research reports[19,20]. The fact was considered that the examined turbulent velocity field was markedly inhomogeneous and anisotropic, while the intensity of turbulence in the investigated stream reached extremely high values, see *e.g.* refs[4–8]. The obtained characteristics of the mean and the fluctuation motion were transformed into the radial, tangential and axial components. The appropriate transformations are summarized in Table II. We note that the expressions for mean velocities can be derived rigorously while the relations for the fluctuation quantities were obtained under certain simplifying assumptions regarding the examined velocity field[3]. *3)* In the concluding stage of experiments with the aid of the quantities $\overline{w}$, $\overline{w'^2}$ and $\overline{u'^2}$ found as just described from the hot-film anemometer data, correlations were evaluated of the longitudinal and lateral fluctuation velocity component $\overline{w'u'}$ using the five-hole Pitot tube (Fig. 4). The method used was a modification of that developed by Jezdinský[19]. The sought turbulent characteristic follows from the solutions

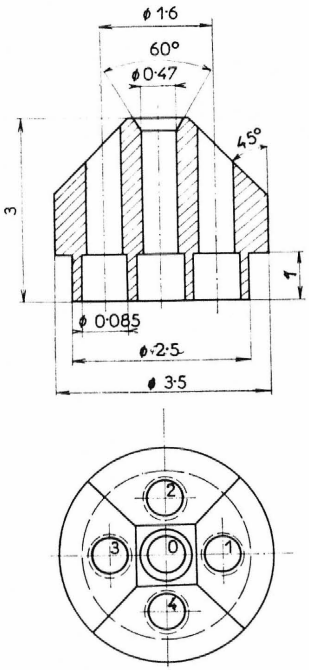

FIG. 3
Five-Hole Directional Pitot Tube

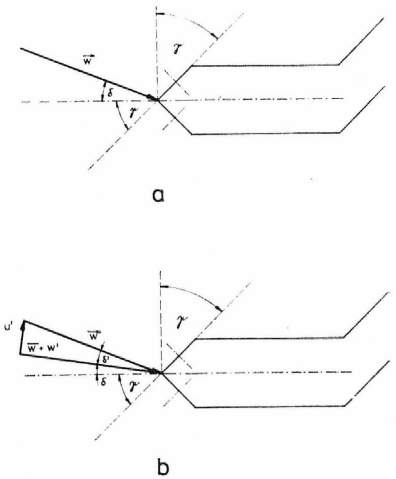

FIG. 4
Directional Pitot Tube in an Incompressible Fluid
a) Potential flow; *b*) turbulent flow.

of equations presented in Table IV. A given i-th opening of the Pitot tube detects the overall pressure in dependence on the angle of tapering γ_i with respect to the axis of the probe, the direction of the vector of instantaneous velocity with respect to the axis of the probe (angle δ) and, finally, on the character of the flow past the probe. If the probe is located in a calibration equipment ensuring potential flow of liquid[18], the directional characteristics of the i-th hole of the probe, A_i, B_i and C_i (Table IV) may be obtained from the calibration curve for each opening, *i.e.* from the dependence $p_{dyn,i} = p_{dyn,i}(w)$. The values of the directional characteristics somewhat differ from the theoretical relations summarized in Table IV because in these equations the size of the i-th opening of the probe is taken to be infinitesimal, which is not true in reality. With the knowledge of the coefficients A_i, B_i and C_i and the in-advance-determined values $\bar{w}$, $\overline{w'^2}$, $\overline{u'^2}$, it is possible to find the mean dynamic pressure $\bar{p}_{dyn,i}$ felt by the i-th opening at the angle of tapering δ of the probe with respect to the direction of mean velocity and the longitudinal fluctuation velocity component and to determine the correlation $\overline{w'u'}$. The mean static pressure $\bar{p}_{st}$ at the measuring point (considered as an invariant) may be determined from the data of the central opening of the probe (designated by zero — see Fig. 3), provided the measurements have been performed for a zero value of the angle δ (see also the appropriate relations in Table IV.). Thus it is possible to evaluate the correlation of the fluctuation velocity components $\overline{w'u'}$ and to transform these into the sought correlation of the components $\overline{u'_p w'_{ax}}$ or $\overline{u'_{tg} u'_{ax}}$ (Table III). It is noted that in each measuring point within the examined jet where the turbulent characteristics were sought, several adjustements of the angle delta of the five-hole Pitot tube were made.

TABLE IV

Characteristics of the Directional Pitot Tube ($i = 0, 1, 2, 3, 4$)

Potential flow

$$p_i = p_{st} + p_{dyn,i} = p_{st} + 1/2\varrho w^2 \cos^2(\delta + \gamma_i)$$

$$p_{dyn,i} = 1/2\varrho w^2 (A_i \sin^2 \delta + B_i \sin \delta \cos \delta + C_i)$$

$$A_i = \sin^2 \gamma_i - \cos^2 \gamma_i\,, \quad B_i = -2 \sin \gamma_i \cos \gamma_i\,, \quad C_i = 1 - \sin^2 \gamma_i$$

Turbulent flow

$$\bar{p}_i = \bar{p}_{st} + \bar{p}_{dyn,i} = \bar{p}_{st} + 1/2\varrho \bar{w}^2 \overline{\cos^2(\delta + \delta' + p_i)}$$

$$\cos \delta' = (\bar{w} + w')/w, \quad \sin \delta' = u'/w\,, \quad w^2 = (\bar{w} + w')^2 + u'^2$$

$$\bar{p}_{dyn,i} = 1/2\bar{w}^2 \{[A_i(1 + \overline{u'^2} - \overline{u'^2}) - 2B_i \overline{w'u'}] \sin^2 \delta +$$

$$+ [B_i(1 + \overline{w'^2}) - A_i(\overline{w'^2} - 2\overline{w'u'})] \sin \delta \cos \delta +$$

$$+ [C_i(1 + \overline{w'^2} + \overline{u'^2}) + A_i \overline{u'^2} + B_i \overline{w'u'})]\}$$

$$\delta = 0^\circ\,; \quad i = 0\,; \quad (\gamma_0 = 0^\circ): \quad A_0 = -1; \quad B_0 = 0\,; \quad C_0 = 1\,;$$

$$\bar{p}_0 = \bar{p}_{st} + \bar{p}_{dyn,0} = \bar{p}_{st} + 1/2\varrho \bar{w}^2 (1 + \overline{w'^2})$$

The quantities $\overline{w'u'}$ were then determined from the reading of that opening which was exposed to the appropriate component of the excess stress tensor, *i.e.* the opening normal was identical with the direction of the stream past the probe. 4—5 values of the angle delta ranging between 3° and 13° were adjusted. Resulting correlation $\overline{w'u'}$ calculated from all measurements in a given point is then arithmetic average from the values for the above apositions of the probe. The spacing of individual measuring points was between 4 and 9 mm in order that each axial profile contain 15 experimental data on average.

RESULTS AND DISCUSSION

The results of the performed experiments were used on the one hand to evaluate the parameters of the proposed theoretical model and, on the other hand, to verify the simplifying assumptions made. The experimentally found velocity field served to the former of the purposes. The found profiles of the mean velocity were processed statistically to yield parameters A_1, A_2 and A_3 of the profiles $\overline{W}_r = \overline{W}_r(Z)$, (Table I) and their dependence on the radial coordinate R. As the radius of the tangential jet, a, was not found in the whole investigated range of arrangements significantly dependent on the ratio d/D. Therefore the experimental results were processed for both arrangements jointly. These results, *i.e.* the dependence of the parameters $A_j = A_j(R)$, $(j = 1, 2, 3)$ are shown in Table I. For the latter of the mentioned purposes of this study we used the turbulent characteristics $\overline{w'_r w'_{ax}}$ whose values can be compared with the theoretical values computed from the equations of the proposed phenomenological model. Similarly we could compare values of the eddy viscosity determined from the theoretical concepts (Table I) and from experiments, that means from the known values of the correlation $\overline{w'_r w'_{ax}}$ and the axial gradient of the radial mean velocity component (Eqs (*1*) and (*2*)). A comparison of the above turbulent characteristics is of importance as a proof of adequacy of the proposed theoretical model; the agreement of the theoretical equations determined from the profiles of the mean velocity component with the results of determination of turbulent characteristics proves consistency of the quasi-stationary description of the turbulent motion in the examined jet stream.

The time-averaged flow in the jet discharging from the space of the rotating turbine impeller represents profiles of the mean velocity or its components in this stream (Figs 5—7). These figures show typical profiles of the velocity or its significant components with the characteristic maximum in the middle of the jet (typical example is illustrated as the radial velocity component in Fig. 5). One can also observe flattening of the profile with increasing radial coordinate. The marked shift of the maximum from the horizontal plane of symmetry upwards is the result of unsymmetric position of the source of mechanical energy (impeller) in the mixed system, characterized by the magnitude of the geometrical simplex $H'_2/H = 1/3$. It cannot go unnoticed that the stream jet widens with increasing radial distance from the impeller. This

occurs owing to the turbulent momentum transfer in the axial direction. The profiles of the tangential mean velocity component display considerable flattening with increasing radial coordinate accompanied by simultaneous overall decrease, which is fully compatible with the concept of cylindrical tangential jet. Axial mean velocity components thus assume small values in comparison with the two remaining ones. This fact confirms the adequacy of the model of the examined jet as being chiefly two-diemensional. The experimentally determined axial profiles of the radial mean velocity component (Fig. 5) yielded through nonlinear regression values of the parameters A_1, A_2, A_3 (Table I) necessary to evaluate, by linear regression, the dependences $A_j = A_j(R)$, $(j = 1, 2, 3)$ – see also Table I. Broken lines in Fig. 5 represent the course of the proposed velocity profiles using the already known values of the parameters A_1, A_2, A_3. The fit of the curves and individual experimental points may be regarded as another proof of adequacy of the proposed model of the flow in the examined stream throughout its length.

The found profiles of the overall intensity of turbulence and its components (Figs 8–11) point out significant inhomogeneity of the stream jet. Individual profiles of the components of intensity of turbulence exhibit deep minima in the center of the jet with a particularly step increase in the vicinity of the rotating blades of the impeller. With increasing radial coordinate the profiles of the components of the intensity of turbulence gradually even out reaching, ultimately, values 20–100% (and more). These values well agree with the discussed turbulent characteristics measured by Cutter[4] and Nielsen[21] by a photographic technique, and by Oldshue[4] and Liepe and

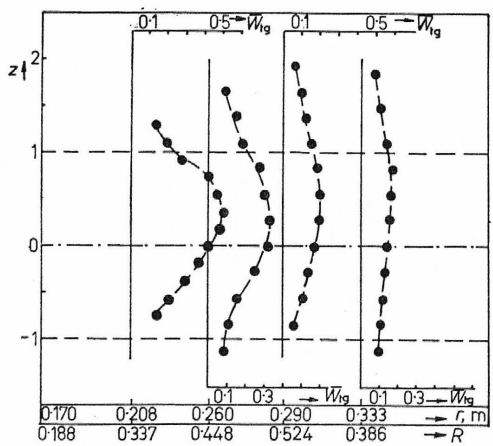

FIG. 5

Axial Profiles of Dimensionless Radial Mean Velocity Component $\overline{W}_r$ ($d/D = 1/3$; $n = 90$ min^{-1})

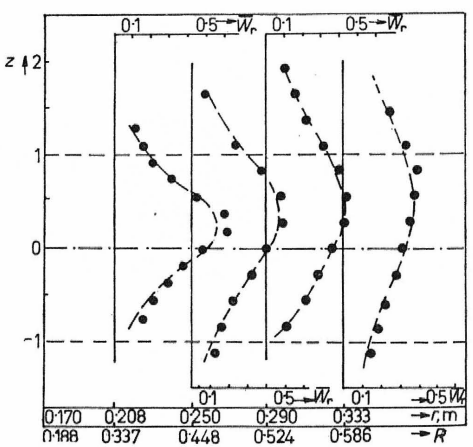

FIG. 6

Axial Profiles of Dimensionless Tangential Mean Velocity Component $\overline{W}_{tg}$ ($d/D = 1/3$; $n = 90$ min^{-1})

coworkers[9] who turned the anemometer probe into the direction of the mean velocity. This has been overlooked by other authors[6,7] and showed through a significant deviation of their results from those of the techniques respecting the sensitivity of the hot-wire probe to the direction of the longitudinal mean and fluxtuation velocity[17] and of the hot-film wedge probe to the longitudinal and lateral mean fluctuation velocity[3,16,18]. From the evaluation of the overall intensity of turbulence and its components in the examined stream it follows that similarly as for the mean velocity and its components one can easily detect the influence of the source of inhomogeneity of the velocity filed, the rotating impeller. Toward the wall of the vessel the profiles of all examined quantities flatten while the level of the overall intensity of turbulence and its components (with the exception of the tangential one, also decaying due to the radial baffles) still exceeds 30%. It is worth noticing that the ratio of the quantities $(\overline{w'^2_{ax}})^{1/2}$ and $\overline{w}_{ax}$ in the examined stream jet did not drop below 100% but usually reached values around 200–800% (and more). The fact that the fluctuation component markedly exceeds corresponding mean velocity may play a role in the estimation of the rate of heat or mass transfer in the discharge jet and in its proximity. It may be inferred that the transfer in the axial direction across the width of the jet would be very intensive, mainly due to turbulent diffusion. The transfer in the other directions (tangential and radial) will take place predominantly through convection due to the time-averaged bulk flow.

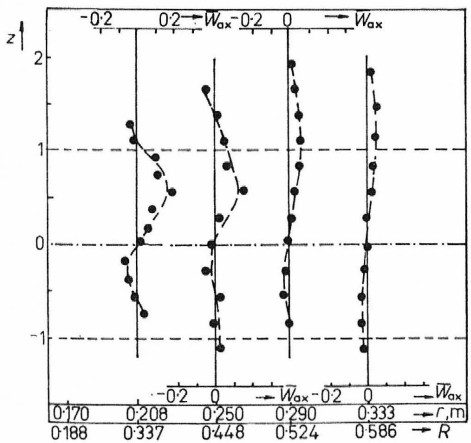

FIG. 7

Axial Profiles of Dimensionless Axial Mean Velocity Component $\overline{W}_{ax}$ ($d/D = 1/3$; $n =$ $= 90\ \text{min}^{-1}$)

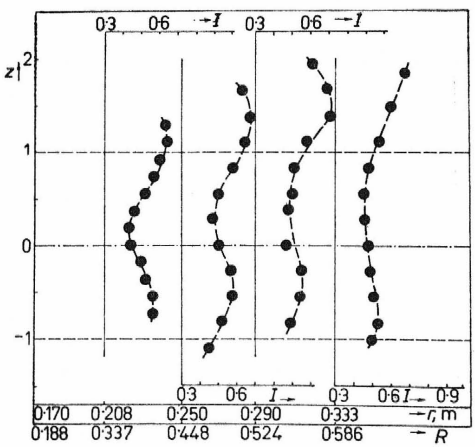

FIG. 8

Axial Profiles of Overall Intensity of Turbulence $I = (\overline{w'^2} + \overline{u'^2})^{1/2}/\overline{w}$ ($d/D = 1/3$; $n =$ $= 90\ \text{min}^{-1}$)

The found profiles of the correlation of fluctuation velocities $\overline{w'_r w'_{ax}}$ (Fig. 12) correspond to the theoretically expected course of these quantities calculated from their relations presented in Table I and considering Eq. (*2*). The axial profile of this correlation depend on the course of axial profile of radial velocity component, that is its derivative with respect to the axial coordinate and takes rather characteristic shape: In the proximity of the limits of the discharge jet for negative axial coordinate (in the bottom part) the absolute value of the quantity $\overline{w'_r w'_{ax}}$ increases to reach maximum about in a quarter of the jet's width. As we approach the point of maximum mean velocity, this quantity decreases to vanish ultimately. Proceeding further to the upper limit of the discharge jet the correlation of the fluctuation components again increase to reach a maximum and again decrease in the proximity of the limits of the discharge jet. With increasing radial coordinate the profiles $\overline{w'_r w'_{ax}}$ even out and their absolute values diminish. These conclusions can be drawn both from the courses of the theoretically found profiles $\overline{W'_r W'_{ax}} = \overline{W'_r W'_{ax}}(Z)$, shown in Fig. 12 by a solid line, and from experimental results, shown by points in this figure. The agreement of the experimental and theoretical values of the correlations is better farther away from the rotating impeller then in its immediate vicinity ($R = 0{\cdot}170$), where the effect of the periodic contribution of the velocity pulsations predominates. Moreover, this effect also changes with the value of the axial coordinate[14]. Thus in this region the proposed phenomenologically model is insatisfactory and its use is limited to that part of the radial coordinate where the contribution of the periodic pulsations becomes

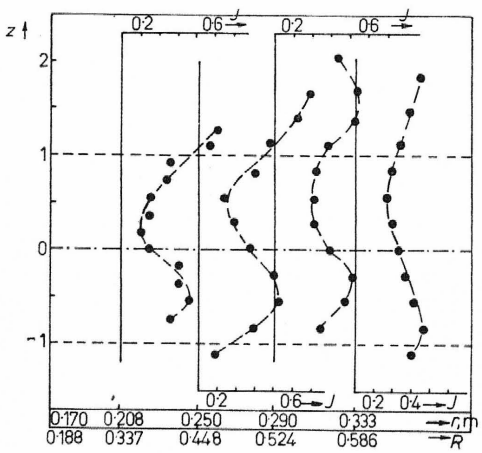

FIG. 9

Axial Profiles of Radial Component of Intensity of Turbulence $J = (\overline{w'^2_r})^{1/2}/w_r$ ($d/D = 1/3$; $n = 90\ \mathrm{min}^{-1}$)

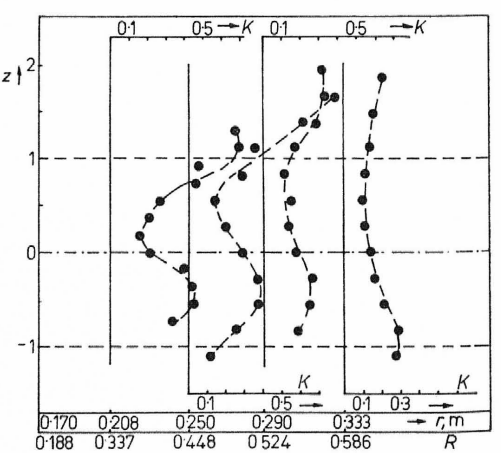

FIG. 10

Axial Profiles of Tangential Component of Intensity of Turbulence $K = (\overline{w'^2_{tg}})^{1/2}/\overline{w}_r$ ($d/D = 1/3$; $n = 90\ \mathrm{min}^{-1}$)

insignificant. From the earlier published papers[6,11] as well as from the found profiles of $\overline{w'_r w'_{ax}}$ it follows that for $R = 0{\cdot}25$ the agreement of the theoretical and experimental data is adequate. Similar conclusion can be made from comparison of the eddy viscosity calculated from the theoretical relationship (Table I) and determined from the found quantity $\overline{w'_r w'_{ax}}$. Combining Eq. (*1*) and Eq. (*2*) we obtain

$$\varepsilon = -\overline{w'_r w'_{ax}} / (\partial \bar{w}_r / \partial z) . \qquad (7)$$

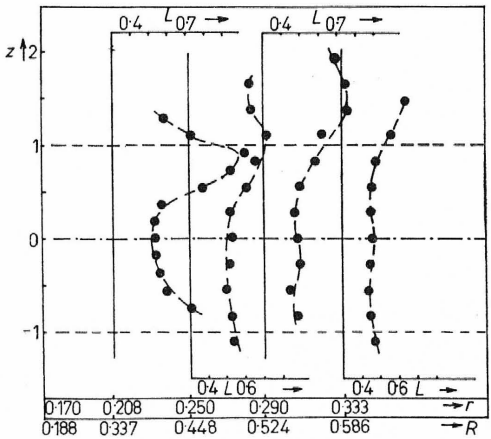

FIG. 11
Axial Profiles of Axial Component of Intensity of Turbulence $L = (\overline{w'^2_{ax}})^{1/2}/\bar{w}_r$ ($d/D = 1/3$; $n = 90\ \mathrm{min}^{-1}$)

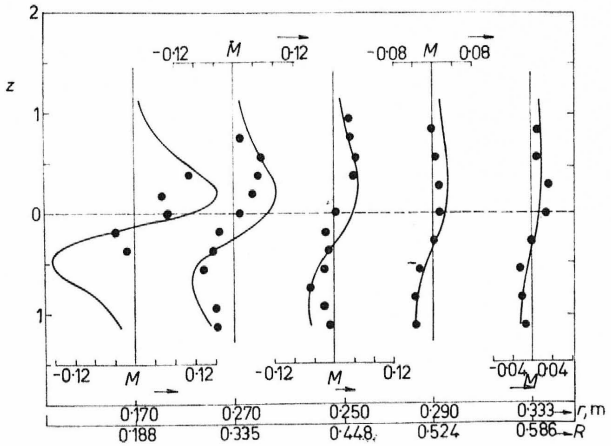

FIG. 12
Axial Profiles of Dimensionless Correlation of Fluctuation Velocity Components $M = \overline{W'_r W'_{ax}}$ ($d/D = 1/3$; $n = 90\ \mathrm{min}^{-1}$)
——— theoretical profiles $\overline{W'_r W'_{ax}} = \overline{W'_r W'_{ax}}(Z)$, ● experimental points $\overline{W'_r W'_{ax}}$.

The derivative of the radial mean velocity component with respect to the axial coordinate can be evaluated by differentiation of the three-parameter theoretical equation, whose parameters A_1, A_2, A_3, had been evaluated by the above described procedure. This may be done thanks to the close fit of the proposed theoretical correlation relation $\overline{W}_r = \overline{W}_r(Z)$. Values of the eddy viscosity determined thus from experimental data and designated ε_m were averaged for the given axial profile and compared with the theoretical values computed for a given r or R from appropriate relation from Table I. From Table V, summarizing these quantities together with the estimate of the standard deviation of ε_m (designated $s_{\varepsilon m}$) it follows that ε and ε_m do not differ with the exception of the first experimental profile by more than 30%. They also do not fulfill the assumptions of the underlying model that ε is to be constant throughout the width of the discharge jet. This, however, is comprehensible considering the fact that the proposed model originates from the classic theory of submerged jets[22,23] discharging from a narrow slot under the potential flow. In our case although the source of motion proper induces marked turbulence with moreover, a periodic component superimposed (due to rotation of the blades). Its energy contribution in the proximity of the rotating impeller is controlling[11,14]. Nevertheless, the found agreement of the theoretical and experimental values of the eddy viscosity may be considered at least as satisfactory and the proposed phenomenological model of the turbulent motion discharging from the space of the rotating turbine impeller may be accepted as valid. The fact that the ratio of the eddy and molecular kinematic viscosity ε/ν in the whole examined jet exceeds $1 \cdot 10^3$ also confirms that the turbulent transfer in this region markedly dominates molecular transport; this fact may be regarded as not only a quantitative proof of the conclusions following from the experimental study of the mass and heat transfer rates in the examined jet[24], but also as a proof of validity of the Reynolds equation in this

TABLE V

Theoretical and Experimental Eddy Viscosities in the Discharge Stream from by the Turbine Impeller (d 0·330 m; $d/D = 1/3$; $n = 90\ \text{min}^{-1}$; $H_1'/H = 1/3$; $H = 1{\cdot}0$ m; water $\nu = 1{\cdot}0 \cdot 10^{-6}\ \text{m}^2\ \text{s}^{-1}$)

r, m; (R)	$\varepsilon \cdot 10^3$, $\text{m}^2\ \text{s}^{-1}$	$\varepsilon_m \cdot 10^3$, $\text{m}^2\ \text{s}^{-1}$	$s_{\varepsilon_m} \cdot 10^3$, $\text{m}^2\ \text{s}^{-1}$
0·170 (0·188)	6·68	4·85	2·7
0·207 (0·335)	5·90	4·65	1·8
0·250 (0·448)	5·40	5·10	3·8
0·290 (0·524)	5·20	4·80	3·3
0·333 (0·586)	5·10	6·10	3·2

region and its solution neglecting viscous stresses with respect to the turbulent ones. Apart from this, it may be expected that the proposed model enables an estimation of the effect of the force field existing in the examined region on the rate of immissible liquid/liquid system droplet disintegration or gas dispergation which in this very region is most intensive and controls the performance of the mixing equipment.

The authors wish to thank Mrs M. Prosková for valuable assistance in preparation of this work.

LIST OF SYMBOLS

A universal parameter of axial profile of radial mean velocity component, $m^2 s^{-1}$
A_j ($j = 1, 2, 3$) parameter of axial profile of radial mean velocity component
A_i ($i = 0, 1, 2, 3, 4$) directional coefficient of the Pitot tube
a radius of cylindrical tangential jet, m
B_i ($i = 0, 1, 2, 3, 4$) directional coefficient of the Pitot tube
b width of radial baffle, m
b_3 constant
C_i ($i = 0, 1, 2, 3, 4$) directional coefficient of the Pitot tube
D vessel diameter, m
d impeller diameter, m
H liquid height at rest, m
H_2' height of the separating disc over bottom, m
h width of impeller's blade, m
n frequence of revolution of impeller, s^{-1}
$\bar{p}_i$ ($i = 0, 1, 2, 3, 4$) mean pressure felt by the i-th opening of the Pitot tube, Pa
$\bar{p}_{st}$ mean local static pressure, Pa
R dimensionless radial distance
r radial coordinate, m
$Re_M = nd^2/\nu$ Reynolds number for mixing
u' fluctuation velocity component perpendicular to the direction of mean velocity, ms^{-1}
W dimensionless mean velocity
W' dimensionless fluctuation velocity
$\overline{W_i' W_j'}$ dimensionless correlation of fluctuation velocity components ($i \neq j$)
$\bar{w}$ mean velocity, ms^{-1}
w' longitudinal fluctuation velocity component, ms^{-1}
$\overline{w_i' w_j'}$ correlation of fluctuation velocity components ($i \neq j$), $m^2 s^{-2}$
Z dimensionless axial coordinate
z axial coordinate, m
α angle
α_0 angular coordinate
β angle
γ angle
δ angle
ε eddy viscosity, $m^2 s^{-1}$
ν molecular kinematic viscosity, $m^2 s^{-1}$
ϱ density, $kg m^{-3}$

σ universal parameter of axial profile of radial mean velocity component
$\bar{\tau}$ turbulent (Reynolds) stress, Pa
φ_j ($j = 1, 2$) directional function of the five-hole Pitot tube
ψ dimensionless stream function

Subscripts

ax axial
i summation index
j summation index
m measured value
r radial
tg tangential

REFERENCES

1. Drbohlav J., Fořt I., Krátký J.: This Journal *43*, 696 (1978).
2. De Souza A., Pike R. W.: Can. J. Chem. Eng. *50*, 15 (1972).
3. Drbohlav J.: *Thesis*. Prague Institute of Chemical Technology, Prague 1975.
4. Cutter L. A.: AIChE J. *12*, 35 (1966).
5. Oldshue J. Y.: Chem. Process. Eng. (Bombay) *183* (April 1966).
6. Mujumdar A. S., Huang B., Wolf D., Weber D., Douglas W. J.: Can J. Chem. Eng. *48*, 457 (1970).
7. Cho S. H., Amarnath P. H., Baker H. A.: Paper presented on the 21st Canadian Chemical Engineering Conference, Montreal 1971.
8. Rao M. A., Brokey R. S.: Chem. Eng. Sci. *27*, 137 (1972).
9. Liepe F., Möckel H. O., Winkler H.: Chem. Techn. (Leipzig) *23*, 231 (1971).
10. Schwartzberg H. G., Treybal R. E.: Ind. Eng. Chem., Fundam. *7*, 1 (1968).
11. Fořt I., Placek J., Durdil P., Drbohlav J., Krátký J.: This Journal *39*, 1810 (1974).
12. Günkel A. A., Weber M. E.: AIChE J. *21*, 931 (1975).
13. Nagata S.: *Mixing*. Kodansha, Tokyo 1975.
14. Van't Riet K., Bruijn W., Smith J. M.: Chem. Eng. Sci. *31*, 407 (1976).
15. Czechoslovak Standard 6910. VÚCHZ — CHEPOS, Brno 1969.
16. Ling S. C.: *Thesis*. State University of Iowa, Iowa 1965.
17. Rasmussen C. G.: DISA Information No. *1*, 1 (1965), No *3*, 9 (1966).
18. Fořt I., Durdil P., Krátký J.: Sb. Vys. Šk. Chemicko-Technol. Praze *K7*, 117 (1975).
19. Jezdinský V.: *Thesis*. Czechoslovak Academy of Sciences, Prague 1964.
20. Krátký J., Drbohlav J., Fořt I.: Unpublished results.
21. Nielsen H. J.: *Thesis*. Illinois Institute of Technology, Illinois 1958.
22. Hinze J. O.: *Turbulence*. McGraw-Hill, New York 1959.
23. Tollmien W.: ZAMM *4*, 468 (1926).
24. Uhl V. W., Gray J. B.: *Mixing*, Vol. I. Academic Press, New York 1966.

Translated by V. Staněk.